

## 3. Mixing in Rivers: Turbulent Diffusion and Dispersion

In previous chapters we considered the processes of advection and molecular diffusion and have seen some example problems with so called “turbulent diffusion” coefficients, where we use the same governing equations, but with larger diffusion (mixing) coefficients. In natural rivers, a host of processes lead to a non-uniform velocity field, which allows mixing to occur much faster than by molecular diffusion alone. In this chapter, we formally derive the equations for non-uniform velocity fields to demonstrate their effects on mixing. First, we consider the effect of a random, turbulent velocity field. Second, we consider the combined effects of diffusion (molecular or turbulent) with a shear velocity profile to develop equations for dispersion. In each case, the resulting equations retain their previous form, but the mixing coefficients are orders of magnitude greater than the molecular diffusion coefficients.

We start by giving a description of turbulence and its effects on the transport of contaminants. We then derive a new advective diffusion equation for turbulent flow and show why turbulence can be described by the regular advective diffusion equation derived previously, but using larger turbulent diffusion coefficients. We then look at the effect of a shear velocity profile on the transport of contaminants and derive one-dimensional equations for longitudinal dispersion. This chapter concludes with a common dye study application to compute the effective mixing coefficients in rivers.

### 3.1 Turbulence and mixing

In the late 1800’s, Reynolds performed a series of experiments on the transport of dye streaks in pipe flow. These were the pioneering observations of turbulence, and his analysis is what gives the  $Re$  number its name. It is interesting to realize that the first contribution to turbulence research was in the area of contaminant transport (the behavior of dye streaks); therefore, we can assume that turbulence has an important influence on transport. In his paper, Reynolds (1883) wrote (taken from Acheson (1990)):

The experiments were made on three tubes. They were all about 4 feet 6 inches [1.37 m] long, and fitted with trumpet mouthpieces, so that water might enter without disturbance. The water was drawn through the tubes out of a large glass tank, in which the tubes were immersed, arrangements being made so that a streak or streaks of highly colored water entered the tubes with the clear water.

The general results were as follows:

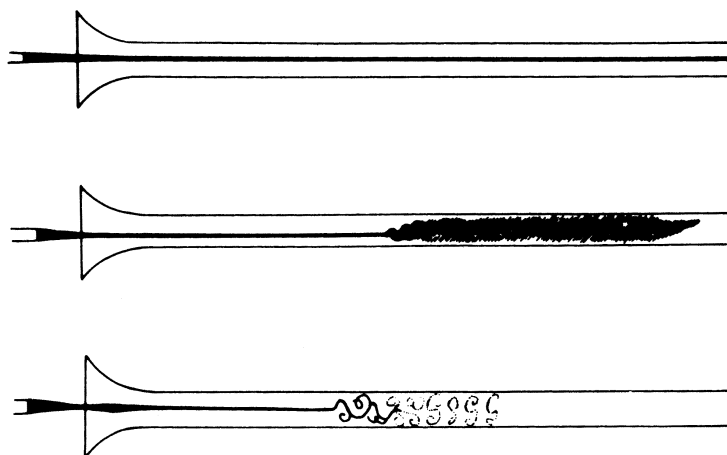


**Fig. 3.1.** Sketches from Reynolds (1883) showing laminar flow (top), turbulent flow (middle), and turbulent flow illuminated with an electric spark (bottom). Taken from Acheson (1990).

1. When the velocities were sufficiently low, the streak of colour extended in a beautiful straight line through the tube.
2. If the water in the tank had not quite settled to rest, at sufficiently low velocities, the streak would shift about the tube, but there was no appearance of sinuosity.
3. As the velocity was increased by small stages, at some point in the tube, always at a considerable distance from the trumpet or intake, the color band would all at once mix up with the surrounding water, and fill the rest of the tube with a mass of colored water. Any increase in the velocity caused the point of break down to approach the trumpet, but with no velocities that were tried did it reach this. On viewing the tube by the light of an electric spark, the mass of color resolved itself into a mass of more or less distinct curls, showing eddies.

Figure 3.1 shows the schematic drawings of what Reynolds saw, taken from his paper.

The first case he describes, the one with low velocities, is laminar flow: the fluid moves in parallel layers along nearly perfect lines, and disturbances are damped by viscosity. The only way that the dye streak can spread laterally in the laminar flow is through the action of molecular diffusion; thus, it would take a much longer pipe before molecular diffusion could disperse the dye uniformly across the pipe cross-section (what rule of thumb could we use to determine the required length of pipe?).

The latter case, at higher velocities, is turbulent flow: the fluid becomes suddenly unstable and develops into a spectrum of eddies, and these disturbances grow due to instability. The dye, which more or less follows the fluid passively, is quickly mixed across the cross-section as the eddies grow and fill the tube with turbulent flow. The observations with an electric spark indicate that the dye conforms to the shape of the eddies. After some time, however, the eddies will have grown and broken enough times that the dye will no longer have strong concentration gradients that outline the eddies: at that point, the

dye is well mixed and the mixing is more or less random (even though it is still controlled by discrete eddies).

Reynolds summarized his results by showing that these characteristics of the flow were dependent on the non-dimensional number  $Re = UL/\nu$ , where  $U$  is the mean pipe flow velocity,  $L$  the pipe diameter and  $\nu$  the kinematic viscosity, and that turbulence occurred at higher values of  $Re$ . The main consequence of turbulence is that it enhances momentum and mass transport.

### 3.1.1 Mathematical descriptions of turbulence

Much research has been conducted in the field of turbulence. The ideas summarized in the following can be found in much greater detail in the treatises by Lumley & Panofsky (1964), Pope (2000), and Mathieu & Scott (2000).

In this section we will consider a special kind of turbulence: homogeneous turbulence. The term homogeneous means that the statistical properties of the flow are steady (unchanging)—the flow can still be highly irregular. These homogeneous statistical properties are usually described by properties of the velocity experienced at a point in space in the turbulent flow (this is an Eulerian description). To understand the Eulerian properties of turbulence, though, it is useful to first consider a Lagrangian frame of reference and follow a fluid particle.

In a turbulent flow, large eddies form continuously and break down into smaller eddies so that there is always a spectrum of eddy sizes present in the flow. As a large eddy breaks down into multiple smaller eddies, very little kinetic energy is lost, and we say that energy is efficiently transferred through a cascade of eddy sizes. Eventually, the eddies become small enough that viscosity takes over, and the energy is damped out and converted into heat. This conversion of kinetic energy to heat at small scales is called dissipation and is designated by

$$\epsilon = \frac{\text{dissipated kinetic energy}}{\text{time}} \quad (3.1)$$

which has the units  $[L^2/T^3]$ . Since the kinetic energy is efficiently transferred down to these small scales, the dissipated kinetic energy must equal the total turbulent kinetic energy of the flow: this means that production and dissipation of kinetic energy in a homogeneous turbulent flow are balanced.

The length scale of the eddies in which turbulent kinetic energy is converted to heat is called the Kolmogorov scale  $L_K$ . How large is  $L_K$ ? We use dimensional analysis to answer this question and recognize that  $L_K$  depends on the rate of dissipation (or, equivalently, production) of energy,  $\epsilon$ , and on the viscosity,  $\nu$ , since friction converts the kinetic energy to heat. Forming a length scale from these parameters, we have

$$L_K \propto \frac{\nu^{3/4}}{\epsilon^{1/4}}. \quad (3.2)$$

This is an important scale in turbulence.

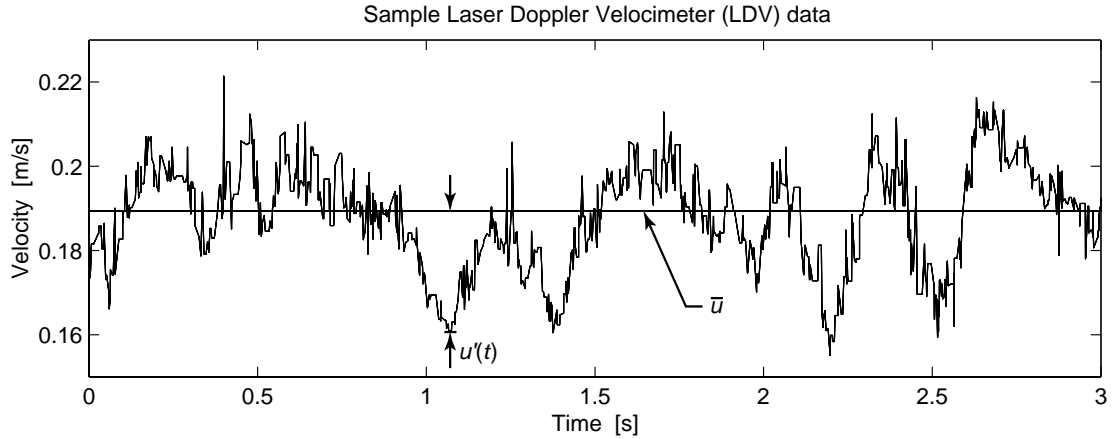


**Fig. 3.2.** Schematic measurement of the turbulent fluctuating velocity at a point showing the average velocity,  $\bar{u}$  and the fluctuating component,  $u'(t)$ .

Summarizing the Lagrangian perspective, if we follow a fluid particle, it may begin by being swept into a large eddy, and then will move from eddy to eddy as the eddies break down, conserving kinetic energy in the cascade. Eventually, the particle finds itself in a small enough eddy (one of order  $L_K$  in size), that viscosity dissipates its kinetic energy into heat. This small eddy is also a part of a larger eddy; hence, all sizes of eddies are present at all times in the flow.

Because it is so difficult to follow a fluid particle with a velocity probe (this is what we try to do with Particle Tracking Velocimetry (PTV)), turbulent velocity measurements are usually made at a point, and turbulence is described by an Eulerian reference frame. The spectrum of eddies pass by the velocity probe, transported with the mean flow velocity. Large eddies produce long-period velocity fluctuations in the velocity measurement, and small eddies produce short-period velocity fluctuations, and all these scales are present simultaneously in the flow. Figure 3.2 shows an example of a turbulent velocity measurement for one velocity component at a point. If we consider a short portion of the velocity measurement, the velocities are highly correlated and appear deterministic. If we compare velocities further apart in the time-series, the velocities become completely uncorrelated and appear random. The time-scale at which velocities begin to appear uncorrelated and random is called the integral time scale  $t_I$ . In the Lagrangian frame, this is the time it takes a parcel of water to forget its initial velocity. This time scale can also be written as a characteristic length and velocity, giving the integral scales  $u_I$  and  $l_I$ .

Reynolds suggested that at some time longer than  $t_I$ , the velocity at a point  $x_i$  could be decomposed into a mean velocity  $\bar{u}_i$  and a fluctuation  $u'_i$  such that

$$u_i(x_i, t) = \bar{u}_i(x_i) + u'_i(x_i, t), \quad (3.3)$$

and this treatment of the velocity is called Reynolds decomposition.  $t_I$  is, then, comparable to the time it takes for  $\bar{u}_i$  to become steady (constant).

One other important descriptor of turbulence is the root-mean-square velocity

$$u_{rms} = \sqrt{\overline{u'u'}} \quad (3.4)$$

which, since kinetic energy is proportional to a velocity squared, is a measure of the turbulent kinetic energy of the flow (i.e. the mean flow kinetic energy is subtracted out since  $u'$  is just the fluctuation from the mean).

### 3.1.2 The turbulent advective diffusion equation

To derive an advective diffusion equation for turbulence, we substitute the Reynolds decomposition into the normal equation for advective diffusion and analyze the results. Before we can do that, we need a Reynolds decomposition analogy for the concentration, namely,

$$C(x_i, t) = \overline{C}(x_i) + C'(x_i, t). \quad (3.5)$$

Since we are only interested in the long-term (long compared to  $t_I$ ) average behavior of a tracer cloud, after substituting the Reynolds decomposition, we will also take a time average. As an example, consider the time-average mass flux in the  $x$ -direction at our velocity probe,  $\overline{uC}$ :

$$\begin{aligned} q_x &= \overline{uC} \\ &= \overline{(\overline{u_i} + u'_i)(\overline{C} + C')} \\ &= \overline{\overline{u_i} \overline{C}} + \overline{\overline{u_i} C'} + \overline{u'_i \overline{C}} + \overline{u'_i C'} \end{aligned} \quad (3.6)$$

where the overbar indicates a time average

$$\overline{uC} = \frac{1}{t_I} \int_t^{t+t_I} uC d\tau. \quad (3.7)$$

For homogeneous turbulence, the average of the fluctuating velocities must be zero,  $\overline{u'_i} = \overline{C'} = 0$ , and we have

$$\overline{uC} = \overline{u_i C} + \overline{u'_i C'} \quad (3.8)$$

where we drop the double over-bar notation since the average of an average is just the average. Note that we cannot assume that the cross term  $\overline{u'_i C'}$  is zero.

With these preliminary tools, we are now ready to substitute the Reynolds decomposition into the governing advective diffusion equation (with molecular diffusion coefficients) as follows

$$\begin{aligned} \frac{\partial C}{\partial t} + \frac{\partial u_i C}{\partial x_i} &= \frac{\partial}{\partial x_i} \left( D \frac{\partial C}{\partial x_i} \right) \\ \frac{\partial (\overline{C} + C')}{\partial t} + \frac{\partial (\overline{u_i} + u'_i)(\overline{C} + C')}{\partial x_i} &= \frac{\partial}{\partial x_i} \left( D \frac{\partial (\overline{C} + C')}{\partial x_i} \right). \end{aligned} \quad (3.9)$$

Next, we integrate over the integral time scale  $t_I$

$$\frac{1}{t_I} \int_t^{t+t_I} \left\{ \frac{\partial (\overline{C} + C')}{\partial \tau} + \frac{\partial (\overline{u_i} + u'_i)(\overline{C} + C')}{\partial x_i} \right\} = \frac{\partial}{\partial x_i} \left( D \frac{\partial (\overline{C} + C')}{\partial x_i} \right) d\tau$$

$$\frac{\partial(\overline{C} + \overline{C'})}{\partial t} + \frac{\partial(\overline{u_i C} + \overline{u_i C'} + \overline{u'_i C} + \overline{u'_i C'})}{\partial x_i} = \frac{\partial}{\partial x_i} \left( D \frac{\partial(\overline{C} + \overline{C'})}{\partial x_i} \right). \quad (3.10)$$

Finally, we recognize that the terms  $\overline{u_i C}$ ,  $\overline{u'_i C}$  and  $\overline{C'}$  are zero, and, after moving the  $\overline{u'_i C'}$ -term to the right hand side, we are left with

$$\frac{\partial \overline{C}}{\partial t} + \overline{u_i} \frac{\partial \overline{C}}{\partial x_i} = - \frac{\partial \overline{u'_i C'}}{\partial x_i} + \frac{\partial}{\partial x_i} \left( D \frac{\partial \overline{C}}{\partial x_i} \right). \quad (3.11)$$

To utilize (3.11), we require a model for the term  $\overline{u'_i C'}$ . Since this term is of the form  $uC$ , we know that it is a mass flux. Since both components of this term are fluctuating, it must be a mass flux associated with the turbulence. Reynolds describes this turbulent component qualitatively as a form of rapid mixing; thus, we might make an analogy with molecular diffusion. Taylor (1921) derived part of this analogy by analytically tracking a cloud of tracer particles in a turbulent flow and calculating the Lagrangian autocorrelation function. His result shows that, for times greater than  $t_I$ , the cloud of tracer particles grows linearly with time. Rutherford (1994) and Fischer et al. (1979) use this result to justify an analogy with molecular diffusion, though it is worth pointing out that Taylor did not take the analogy that far. For the diffusion analogy model, the average turbulent diffusion time step is  $\Delta t = t_I$ , and the average turbulent diffusion length scale is  $\Delta x = u_I t_I = l_I$ ; hence, the model is only valid for times greater than  $t_I$ . Using a Fick's law type relationship for turbulent diffusion gives

$$\overline{u'_i C'} = D_t \frac{\partial \overline{C}}{\partial x_i} \quad (3.12)$$

with

$$\begin{aligned} D_t &= \frac{(\Delta x)^2}{\Delta t} \\ &= u_I l_I. \end{aligned} \quad (3.13)$$

Substituting this model for the average turbulent diffusive transport into (3.11) and dropping the overbar notation gives

$$\frac{\partial C}{\partial t} + u_i \frac{\partial C}{\partial x_i} = \frac{\partial}{\partial x_i} \left( D_t \frac{\partial C}{\partial x_i} \right) + \frac{\partial}{\partial x_i} \left( D_m \frac{\partial C}{\partial x_i} \right). \quad (3.14)$$

As we will see in the next section,  $D_t$  is usually much greater than the molecular diffusion coefficient  $D_m$ ; thus, the final term is typically neglected.

### 3.1.3 Turbulent diffusion coefficients in rivers

So, how big are these turbulent diffusion coefficients? To answer this question, we need to determine what the coefficients depend on and use dimensional analysis.

For this purpose, consider a wide river with depth  $h$  and width  $W \gg h$ . An important property of three-dimensional turbulence is that the largest eddies are usually limited by the smallest spatial dimension, in this case, the depth. This means that turbulent

**Example Box 3.1:**

**Turbulent diffusion in a room.**

To demonstrate turbulent diffusion in a room, a professor sprays a point source of perfume near the front of a lecture hall. The room dimensions are 10 m by 10 m by 5 m, and there are 50 people in the room. How long does it take for the perfume to spread through the room by turbulent diffusion?

To answer this question, we need to estimate the air velocity scales in the room. Each person represents a heat source of 60 W; hence, the air flow in the room is dominated by convection. The vertical buoyant velocity  $w_*$  is, by dimensional analysis,

$$w_* = (BL)^{1/3}$$

where  $B$  is the buoyancy flux per unit area in  $[L^2/T^3]$  and  $L$  is the vertical dimension of the room (here 5 m). The buoyancy of the air increases with temperature due to expansion. The net buoyancy flux per unit area is given by

$$B = \beta g \frac{H}{\rho c_v}$$

where  $\beta$  is the coefficient of thermal expansion ( $0.00024 \text{ K}^{-1}$  for air),  $H$  is the heat flux per unit area,  $\rho$  is the density ( $1.25 \text{ kg/m}^3$  for air), and  $c_v$  is the specific heat at constant volume ( $1004 \text{ J/(Kg}\cdot\text{K)}$  for air).

For this problem,

$$\begin{aligned} H &= \frac{50 \text{ pers.} \cdot 60 \text{ W/pers.}}{10^2 \text{ m}^2} \\ &= 30 \text{ W/m}^2. \end{aligned}$$

This gives a unit area buoyancy flux of  $5.6 \cdot 10^{-5} \text{ m}^2/\text{s}^3$  and a vertical velocity of  $w_* = 0.07 \text{ m/s}$ .

We now have the necessary scales to estimate the turbulent diffusion coefficient from (3.13). Taking  $u_I \propto w_*$  and  $l_I \propto h$ , where  $h$  is the height of the room,

$$\begin{aligned} D_t &\propto w_* h \\ &\approx 0.35 \text{ m}^2/\text{s} \end{aligned}$$

which is much greater than the molecular diffusion coefficient (compare to  $D_m = 10^{-5} \text{ m}^2/\text{s}$  in air). The mixing time can be taken from the standard deviation of the cloud width

$$t_{mix} \approx \frac{L^2}{D_t}$$

For vertical mixing,  $L = 5 \text{ m}$ , and  $t_{mix}$  is 1 minute; for horizontal mixing,  $L = 10 \text{ m}$ , and  $t_{mix}$  is 5 minutes. Hence, it takes a few minutes (not just a couple seconds or a few hours) for the students to start to smell the perfume.

properties in a wide river should be independent of the width, but dependent on the depth. Also, turbulence is thought to be generated in zones of high shear, which in a river would be at the bed. A parameter that captures the strength of the shear (and also is known to be proportional to many turbulent properties) is the shear velocity  $u_*$  defined as

$$u_* = \sqrt{\frac{\tau_0}{\rho}} \tag{3.15}$$

where  $\tau_0$  is the bed shear and  $\rho$  is the fluid density. For uniform open channel flow, the shear friction is balanced by gravity, and

$$u_* = \sqrt{gdS} \tag{3.16}$$

where  $S$  is the channel slope. Arranging our two parameters ( $d$  and  $u_*$ ) to form a diffusion coefficient gives

$$D_t \propto u_* d. \tag{3.17}$$

Because the velocity profile is much different in the vertical ( $z$ ) direction as compared with the transverse ( $y$ ) direction,  $D_t$  is not expected to be isotropic (i.e. it is not the same in all directions).

**Vertical mixing.** Vertical turbulent diffusion coefficients can be derived from the velocity profile (see Fischer et al. (1979)). For fully developed turbulent open-channel flow, it can be shown that the average turbulent log-velocity profile is given by

$$\overline{u_t}(z) = \overline{u} + \frac{u_*}{\kappa}(1 + \ln(z/d)) \quad (3.18)$$

where  $\kappa$  is the von Karman constant. Taking  $\kappa = 0.4$ , we obtain

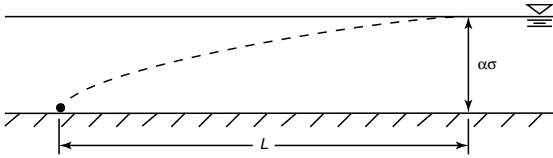
$$D_{t,z} = 0.067du_*. \quad (3.19)$$

This relationship has been verified by experiments for rivers and for atmospheric boundary layers and can be considered accurate to  $\pm 25\%$ .

### Example Box 3.2:

Vertical mixing in a river.

A factory wastestream is introduced through a lateral diffuser at the bed of a river, as shown in the following sketch.



At what distance downstream can the injection be considered as fully mixed in the vertical?

The assumption of “fully mixed” can be defined as the condition where concentration variations over the cross-section are below a threshold criteria. Since the vertical domain has two boundaries, we have to use an image-source solution similar to (2.47) to compute the concentration distribution. The results can be summarized by determining the appropriate value of  $\alpha$  in the relationship

$$h = \alpha\sigma$$

where  $h$  is the depth and  $\sigma$  is the standard deviation of the concentration distribution. Fischer et al. (1979) suggest  $\alpha = 2.5$ .

For vertical mixing, we are interested in the vertical turbulent diffusion coefficient, so we can write

$$h = 2.5\sqrt{2D_{t,z}t}$$

where  $t$  is the time required to achieve vertical mixing. Over the time  $t$ , the plume travels downstream a distance  $L = \overline{u}t$ . We can also make the approximation  $u_* = 0.1\overline{u}$ . Substituting these relationships together with (3.19) gives

$$h = 2.5\sqrt{2 \cdot 0.067h(0.1\overline{u})L/\overline{u}}.$$

Solving for  $L$  gives

$$L = 12h.$$

Thus, a bottom or surface injection in a natural stream can be treated as fully vertically mixed after a distance of approximately 12 times the channel depth.

**Transverse mixing.** On average there is no transverse velocity profile and mixing coefficients must be obtained from experiments. For a wealth of laboratory and field experiments reported in Fischer et al. (1979), the average transverse turbulent diffusion coefficient in a uniform straight channel can be taken as

$$D_{t,y} = 0.15du_*. \quad (3.20)$$

The experiments indicate that the width plays some role in transverse mixing; however, it is unclear how that effect should be incorporated (Fischer et al. 1979). Transverse mixing deviates from the behavior in (3.20) primarily due to large, coherent lateral motions, which are really not properties of the turbulence in the first place. Based on the ranges reported in the experiments, (3.20) should be considered accurate to at best  $\pm 50\%$ .

In natural streams, the cross-section is rarely of uniform depth, and the fall-line tends to meander. These two effects enhance transverse mixing, and for natural streams, Fischer et al. (1979) suggest the relationship

$$D_{t,y} = 0.6du_*. \quad (3.21)$$

If the stream is slowly meandering and the side-wall irregularities are moderate, the coefficient in (3.21) is usually found in the range 0.4–0.8.

**Longitudinal mixing.** Since we assume there are no boundary effects in the lateral or longitudinal directions, longitudinal turbulent mixing should be equivalent to transverse mixing:

$$D_{t,x} = D_{t,y}. \quad (3.22)$$

However, because of non-uniformity of the vertical velocity profile and other non-uniformities (dead zones, curves, non-uniform depth, etc.) a process called longitudinal dispersion dominates longitudinal mixing, and  $D_{t,x}$  can often be neglected, with a longitudinal dispersion coefficient (derived in the next section) taking its place.

**Summary.** For a natural stream with width  $W = 10$  m, depth  $h = 0.3$  m, flow rate  $Q = 1$  m<sup>3</sup>/s, and slope  $S = 0.0005$ , the relationships (3.19), (3.20), and (3.22) give

$$D_{t,z} = 6.4 \cdot 10^{-4} \text{ m}^2/\text{s} \quad (3.23)$$

$$D_{t,y} = 5.7 \cdot 10^{-3} \text{ m}^2/\text{s} \quad (3.24)$$

$$D_{t,x} = 5.7 \cdot 10^{-3} \text{ m}^2/\text{s}. \quad (3.25)$$

Since these calculations show that  $D_t$  in natural streams is several orders of magnitude greater than the molecular diffusion coefficient, we can safely remove  $D_m$  from (3.14).

## 3.2 Longitudinal dispersion

In the previous section we saw that turbulent fluctuating velocities caused a kind of random mixing that could be described by a Fickian diffusion process with larger, turbulent diffusion coefficients. In this section we want to consider what effect velocity deviations in space, due to non-uniform velocity, or shear-flow, profiles, might have on the transport of contaminants.

Figure 3.3 depicts schematically what happens to a dye patch in a shear flow such as open-channel flow. If we inject a contaminant so that it is uniformly distributed across the cross-section at point (a), there will be no vertical concentration gradients and, therefore, no net diffusive flux in the vertical at that point. The patch of tracer will advect downstream and get stretched due to the different advection velocities in the shear profile. After some short distance downstream, the patch will look like that at point (b). At that point there are strong vertical concentration gradients, and therefore, a large net diffusive flux in the vertical. As the stretched out patch continues downstream, (turbulent) diffusion will smooth out these vertical concentration gradients, and far enough downstream, the patch will look like that at point (c). The amount that the patch has spread out in the downstream direction at point (c) is much more than what could have been produced by just longitudinal (turbulent) diffusion. This combined process of advection and lateral diffusion is called dispersion.

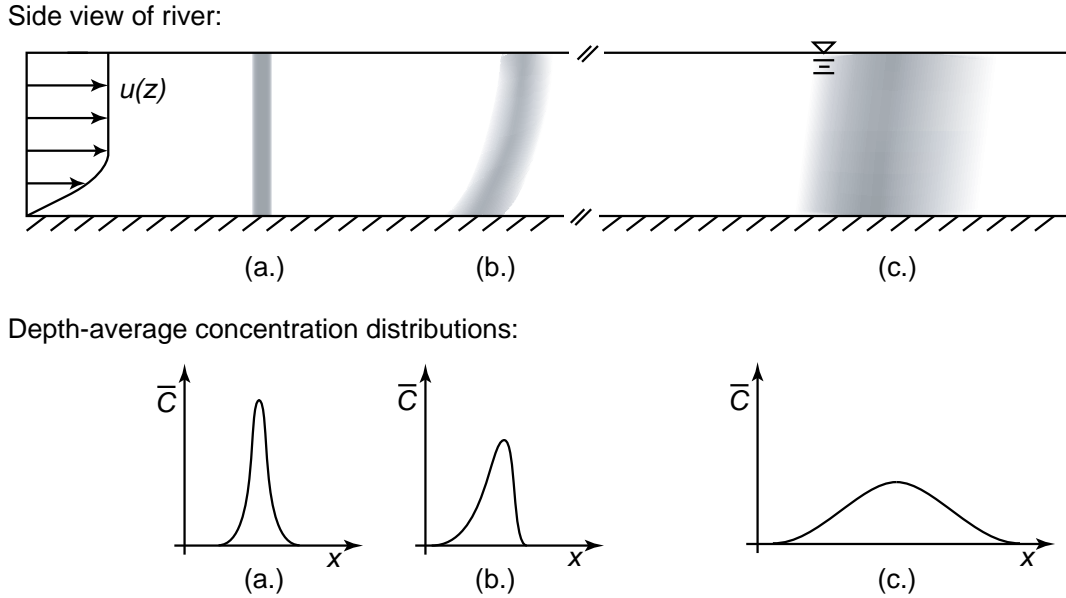


**Fig. 3.3.** Schematic showing the process of longitudinal dispersion. Tracer is injected uniformly at (a) and stretched by the shear profile at (b). At (c) vertical diffusion has homogenized the vertical gradients and a depth-averaged Gaussian distribution is expected in the concentration profiles.

If we solve the transport equation in three dimensions using the appropriate molecular or turbulent diffusion coefficients, we do not need to do anything special to capture the stretching effect of the velocity profile described above. Dispersion is implicitly included in three-dimensional models.

However, we would like to take advantage of the fact that the concentration distribution at the point (c.) is essentially one-dimensional: it is well mixed in the  $y$ - and  $z$ -directions. In addition, the concentration distribution at point (c) is observed to be Gaussian, suggesting a Fickian-type diffusive process. Taylor's analysis for dispersion, as presented in the following, is a method to include the stretching effects of dispersion in a one-dimensional model. The result is a one-dimensional transport equation with an enhanced longitudinal mixing coefficient, called the longitudinal dispersion coefficient.

As pointed out by Fischer et al. (1979), the analysis presented by G. I. Taylor to compute the longitudinal dispersion coefficient from the shear velocity profile is a particularly impressive example of the genius of G. I. Taylor. At one point we will cancel out the terms of the equation for which we are trying to solve. Through a scale analysis we will discard terms that would be difficult to evaluate. And by thoroughly understanding the physics of the problem, we will use a steady-state assumption that will make the problem tractable. Hence, just about all of our mathematical tools will be used.

### 3.2.1 Derivation of the advective dispersion equation

To derive an equation for longitudinal dispersion, we will follow a modified version of the Reynolds decomposition introduced in the previous section to handle turbulence. Referring to Figure 3.4, we see that for one component of the turbulent decomposition,

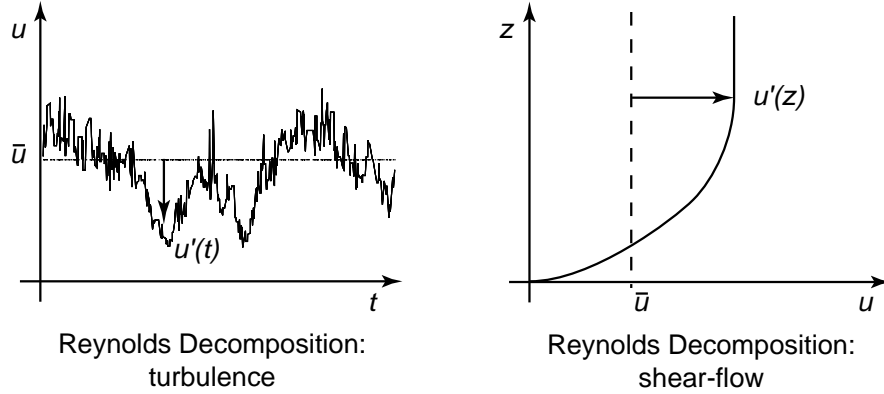


**Fig. 3.4.** Comparison of the Reynolds decomposition for turbulent flow (left) and shear flow (right).

we have a mean velocity that is constant at a point  $x_i$  in three dimensional space and fluctuating velocities that are variable in time so that

$$u(x_i, t) = \bar{u}(x_i) + u'(x_i, t). \quad (3.26)$$

For shear-flow decomposition (here, we show the log-velocity profile in a river), we have a mean velocity that is constant over the depth and deviating velocities that are variable over the depth such that

$$u(z) = \bar{u} + u'(z) \quad (3.27)$$

where the overbar represents a depth average, not an average of turbulent fluctuations. We explicitly assume that  $\bar{u}$  and  $u'(z)$  are independent of  $x$ . A main difference between these two equations is that (3.26) has a random fluctuating component  $u'(x_i, t)$ ; whereas, (3.27) has a deterministic, non-random (and fully known!) fluctuating component  $u'(z)$ , which we rather call a deviation than a fluctuation. As for turbulent diffusion above, we also have a Reynolds decomposition for the concentrations

$$C(x, z) = \bar{C}(x) + C'(x, z) \quad (3.28)$$

which is dependent on  $x$ , and for which  $C'(x, z)$  is unknown.

Armed with these concepts, we are ready to follow Taylor's analysis and apply it to longitudinal dispersion in an open channel. For this derivation we will assume laminar flow and an infinitely wide channel with no-flux boundaries at the top and bottom, so that  $v = w = 0$ . The dye patch is introduced as a plane so that we can neglect lateral diffusion ( $\partial C / \partial y = 0$ ). The governing advective diffusion equation is

$$\frac{\partial C}{\partial t} + u \frac{\partial C}{\partial x} = D_x \frac{\partial^2 C}{\partial x^2} + D_z \frac{\partial^2 C}{\partial z^2}. \quad (3.29)$$

This equation is valid in three dimensions and contains the effect of dispersion. The diffusion coefficients would either be molecular or turbulent, depending on whether the flow is laminar or turbulent. Substituting the Reynolds decomposition for the shear velocity profile, we obtain

$$\frac{\partial(\bar{C} + C')}{\partial t} + (\bar{u} + u') \frac{\partial(\bar{C} + C')}{\partial x} = D_x \frac{\partial^2(\bar{C} + C')}{\partial x^2} + D_z \frac{\partial^2(\bar{C} + C')}{\partial z^2}. \quad (3.30)$$

Since we already argued that longitudinal dispersion will be much greater than longitudinal diffusion, we will neglect the  $D_x$ -term for brevity (it can always be added back later as an additive diffusion term). Also, note that  $\bar{C}$  is not a function of  $z$ ; thus, it drops out of the final  $D_z$ -term.

As usual, it is easier to deal with this equation in a frame of reference that moves with the mean advection velocity; thus, we introduce the coordinate transformation

$$\xi = x - \bar{u}t \quad (3.31)$$

$$\tau = t \quad (3.32)$$

$$z = z, \quad (3.33)$$

and using the chain rule, the differential operators become

$$\begin{aligned} \frac{\partial}{\partial x} &= \frac{\partial}{\partial \xi} \frac{\partial \xi}{\partial x} + \frac{\partial}{\partial \tau} \frac{\partial \tau}{\partial x} + \frac{\partial}{\partial z} \frac{\partial z}{\partial x} \\ &= \frac{\partial}{\partial \xi} \end{aligned} \quad (3.34)$$

$$\begin{aligned} \frac{\partial}{\partial t} &= \frac{\partial}{\partial \xi} \frac{\partial \xi}{\partial t} + \frac{\partial}{\partial \tau} \frac{\partial \tau}{\partial t} + \frac{\partial}{\partial z} \frac{\partial z}{\partial t} \\ &= \frac{\partial}{\partial \tau} - \bar{u} \frac{\partial}{\partial \xi} \end{aligned} \quad (3.35)$$

$$\begin{aligned} \frac{\partial}{\partial z} &= \frac{\partial}{\partial \xi} \frac{\partial \xi}{\partial z} + \frac{\partial}{\partial \tau} \frac{\partial \tau}{\partial z} + \frac{\partial}{\partial z} \frac{\partial z}{\partial z} \\ &= \frac{\partial}{\partial z}. \end{aligned} \quad (3.36)$$

Substituting this transformation and combining like terms (and dropping the terms discussed above) we obtain

$$\frac{\partial(\bar{C} + C')}{\partial \tau} + \frac{\partial u'(\bar{C} + C')}{\partial \xi} = D_z \frac{\partial^2 C'}{\partial z^2}, \quad (3.37)$$

which is effectively our starting point for Taylor's analysis.

The discussion above indicates that it is the gradients of concentration and velocity in the vertical that are responsible for the increased longitudinal dispersion. Thus, we would like, at this point, to remove the non-fluctuating terms (terms without a prime) from (3.37). This step takes great courage and profound foresight, since that means getting rid of  $\partial\bar{C}/\partial t$ , which is the quantity we would ultimately like to predict (Fischer et al. 1979). As we will see, however, this is precisely what enables us to obtain an equation for the dispersion coefficient.

To remove the constant components from (3.37), we will take the depth average of (3.37) and then subtract that result from (3.37). The depth-average operator is

$$\frac{1}{h} \int_0^h dz. \quad (3.38)$$

Applying the depth average to (3.37) leaves

$$\frac{\partial \bar{C}}{\partial \tau} + \frac{\partial \overline{u' C'}}{\partial \xi} = 0, \quad (3.39)$$

since the depth average of  $C'$  is zero, but the cross-term,  $\overline{u' C'}$ , may not be zero. This equation is the one-dimensional governing equation we are looking for. We will come back to this equation once we have found a relationship for  $\overline{u' C'}$ . Subtracting this result from (3.37), we obtain

$$\frac{\partial C'}{\partial \tau} + u' \frac{\partial \bar{C}}{\partial \xi} + u' \frac{\partial C'}{\partial \xi} = \frac{\partial \overline{u' C'}}{\partial \xi} + D_z \frac{\partial^2 C'}{\partial z^2}, \quad (3.40)$$

which gives us a governing equation for the concentration deviations  $C'$ . If we can solve this equation for  $C'$ , then we can substitute the solution into (3.39) to obtain the desired equation for  $\bar{C}$ .

Before we solve (3.40), let us consider the scale of each term and decide whether it is necessary to keep all the terms. This is called a scale-analysis. We are seeking solutions for the point (c) in Figure 3.3. At that point, a particle in the cloud has thoroughly sampled the velocity profile, and  $C' \ll \bar{C}$ . Thus,

$$u' \frac{\partial C'}{\partial \xi} \ll u' \frac{\partial \bar{C}}{\partial \xi} \quad \text{and} \quad (3.41)$$

$$\frac{\partial \overline{u' C'}}{\partial \xi} \ll u' \frac{\partial \bar{C}}{\partial \xi}. \quad (3.42)$$

We can neglect the two terms on the left-hand-side of the inequalities above, leaving us with

$$\frac{\partial C'}{\partial \tau} + u' \frac{\partial \bar{C}}{\partial \xi} = D_z \frac{\partial^2 C'}{\partial z^2}. \quad (3.43)$$

This might be another surprise. In the turbulent diffusion case, it was the cross-term  $\overline{u' C'}$  that became our turbulent diffusion term. Here, we have just discarded this term. In turbulence (as will also be the case here for dispersion), that cross-term represents mass transport due to the fluctuating velocities. But let us, also, take a closer look at the middle term of (3.43). This term is an advection term working on the mean concentration,  $\bar{C}$ , but due to the non-random deviating velocity,  $u'(z)$ . Thus, it is the transport term that represents the action of the shear velocity profile.

Next, we see another insightful simplification that Taylor made. In the beginning stages of dispersion ((a) and (b) in Figure 3.3) the concentration fluctuations are unsteady, but downstream (at point (c)), after the velocity profile has been thoroughly sampled, the vertical concentration fluctuations will reach a steady state (there will be a balanced vertical transport of contaminant), which represents the case of a constant (time-invariant) dispersion coefficient. At steady state, (3.43) becomes

$$u' \frac{\partial \bar{C}}{\partial \xi} = \frac{\partial}{\partial z} \left( D_z \frac{\partial C'}{\partial z} \right) \quad (3.44)$$

where we have written the form for a non-constant  $D_z$ . Solving for  $C'$  by integrating twice gives

$$C'(z) = \frac{\partial \bar{C}}{\partial \xi} \int_0^z \frac{1}{D_z} \int_0^z u' dz dz, \quad (3.45)$$

which looks promising, but still contains the troublesome  $\bar{C}$ -term.

Let's step back for a moment and consider what the mass flux in the longitudinal direction is. In our moving coordinate system, we only have one velocity; thus, the advective mass flux must be

$$q_a = u'(\bar{C} + C'). \quad (3.46)$$

To obtain the total mass flux, we take the depth average

$$\begin{aligned} \bar{q}_a &= \frac{1}{h} \int_0^h u'(\bar{C} + C') dz \\ &= \frac{1}{h} \int_0^h u' C' dz \\ &= \overline{u' C'}. \end{aligned} \quad (3.47)$$

Recall that the depth average of  $u' \bar{C}$  is zero. Substituting the solution for  $C'$  from (3.45), the depth-average mass flux becomes

$$\bar{q}_a = \frac{1}{h} \int_0^h u' \frac{\partial \bar{C}}{\partial \xi} \int_0^z \frac{1}{D_z} \int_0^z u' dz dz dz. \quad (3.48)$$

We can take  $\partial \bar{C} / \partial \xi$  outside of the integral since it is independent of  $z$ , leaving us with

$$\bar{q}_a = -D_L \frac{\partial \bar{C}}{\partial \xi} \quad (3.49)$$

where

$$D_L = -\frac{1}{h} \int_0^h u' \int_0^z \frac{1}{D_z} \int_0^z u' dz dz dz, \quad (3.50)$$

and we have a Fick's law-type mass flux relationship in (3.49). Since the equation for  $D_L$  is just a function of the depth and the velocity profile, we can calculate  $D_L$  for any velocity profile by integrating; thus, we have an analytical solution for the longitudinal dispersion coefficient.

The final step is to introduce this result into the depth-average governing equation (3.39) to obtain

$$\frac{\partial \bar{C}}{\partial \tau} = \frac{\partial}{\partial \xi} \left( D_L \frac{\partial \bar{C}}{\partial \xi} \right), \quad (3.51)$$

which, in the original coordinate system, gives the one-dimensional advective dispersion equation

$$\frac{\partial \bar{C}}{\partial t} + \bar{u} \frac{\partial \bar{C}}{\partial x} = \frac{\partial}{\partial x} \left( D_L \frac{\partial \bar{C}}{\partial x} \right) \quad (3.52)$$

with  $D_L$  as defined by (3.50).

**Example Box 3.3:****River mixing processes.**

As part of a dye study to estimate the mixing coefficients in a river, a student injects a slug (point source) of dye at the surface of a stream in the middle of the cross-section. Discuss the mixing processes and the length scales affecting the injected tracer.

Although the initial vertical momentum of the dye injection generally results in good vertical mixing, assume here that the student carefully injects the dye just at the stream surface. Vertical turbulent diffusion will mix the dye over the depth, and from Example Box 3.2 above, the injection can be treated as mixed in the vertical after the point

$$L_z = 12h$$

where  $h$  is the stream depth.

As the dye continues to move downstream, lateral turbulent diffusion mixes the dye in the transverse direction. Based on the discussion in Example Box 3.2, the tracer can be considered well mixed laterally after

$$L_y = \frac{W^2}{3h}$$

where  $W$  is the stream width.

For the region between the injection and  $L_z$ , the dye cloud is fully three-dimensional, and no simplifications can be made to the transport equation. Beyond  $L_z$ , the cloud is vertically mixed, and longitudinal dispersion can be applied. For distances less than  $L_y$ , a two-dimensional model with lateral turbulent diffusion and longitudinal dispersion is required. For distances beyond  $L_y$ , a one-dimensional longitudinal dispersion model is acceptable.

**3.2.2 Calculating longitudinal dispersion coefficients**

All the brilliant mathematics in the previous section really paid off since we ended up with an analytical solution for the dispersion coefficient

$$D_L = -\frac{1}{h} \int_0^h u' \int_0^z \frac{1}{D_z} \int_0^z u' dz dz dz.$$

In real streams, it is usually the lateral shear (in the  $y$ -direction) rather than the vertical shear that plays the more important role. For lateral shear, Fischer et al. (1979) derive by a similar analysis the relationship

$$D_L = -\frac{1}{A} \int_0^W u' h \int_0^y \frac{1}{D_z h} \int_0^y u' h dy dy dy \quad (3.53)$$

where  $A$  is the cross-sectional area of the stream and  $W$  is the width. Irrespective of which relationship we choose, the question that remains is, how do we best calculate these integrals.

**Analytical solutions.** For laminar flows, analytical velocity profiles may sometimes exist and (3.50) can be calculated analytically. Following examples in Fischer et al. (1979), the simplest flow is the flow between two infinite plates, where the top plate is moving at  $U$  relative to the bottom plate. For that case

$$D_L = \frac{U^2 d^2}{120 D_z} \quad (3.54)$$

where  $d$  is the distance between the two plates. Similarly, for laminar pipe flow, the solution is

$$D_L = \frac{a^2 U_0^2}{192 D_r} \quad (3.55)$$

where  $a$  is the pipe radius,  $U_0$  is the pipe centerline velocity and  $D_r$  is the radial diffusion coefficient.

For turbulent flow, an analysis similar to the section on turbulent diffusion can be carried out and the result is that (3.50) keeps the same form, and we substitute the turbulent diffusion coefficient and the mean turbulent shear velocity profile for  $D_z$  and  $u'$ . The result for turbulent flow in a pipe becomes

$$D_L = 10.1au_*. \quad (3.56)$$

One result of particular importance is that for an infinitely wide open channel of depth  $h$ . Using the log-velocity profile (3.18) with von Karman constant  $\kappa = 0.4$  and the relationship (3.50), the dispersion coefficient is

$$D_L = 5.93hu_*. \quad (3.57)$$

Comparing this equation to the prediction for longitudinal turbulent diffusion from the previous section ( $D_{t,x} = 0.15hu_*$ ) we see that  $D_L$  has the same form ( $\propto hu_*$ ) and that  $D_L$  is indeed much greater than longitudinal turbulent diffusion. For real open channels, the lateral shear velocity profile between the two banks becomes dominant and the leading coefficient for  $D_L$  can range from 5 to 7000 (Fischer et al. 1979). For further discussion of analytical solutions, see Fischer et al. (1979).

**Numerical integration.** In many practical engineering applications, the variable channel geometry makes it impossible to assume an analytical shear velocity profile. In that case, one alternative is to break the river cross-section into a series of bins, measure the mean velocity in each bin, and then compute the second relationship (3.53) by numerical integration. Fischer et al. (1979) give a thorough discussion of how to do this.

**Engineering estimates.** When only very rough measurements are available, it is necessary to come up with a reasonably accurate engineering estimate for  $D_L$ . To do this, we first write (3.53) in non-dimensional form using the dimensionless variables (denoted by  $*$ ) defined by

$$y = Wy^*; \quad u' = \sqrt{\overline{u'^2}}u'^*; \quad D_y = \overline{D_y}D_y^*; \quad h = \bar{h}h^*$$

where the overbar indicates a cross-sectional average. As we already said, longitudinal dispersion in streams is dominated by the lateral shear velocity profile, which is why we are using  $y$  and  $D_y$ . Substituting this non-dimensionalization into (3.53) we obtain

$$D_L = \frac{W^2\overline{u'^2}}{\overline{D_y}}I \quad (3.58)$$

where

$$I = - \int_0^1 u'^*h^* \int_0^{y^*} \frac{1}{D_y^*h^*} \int_0^{y^*} u'^*h^* dy^* dy^* dy^*. \quad (3.59)$$

As Fischer et al. (1979) point out, in most practical cases it may suffice to take  $I \approx 0.01$  to  $0.1$ .

To go one step further, we introduce some further scales measured by Fischer et al. (1979). From experiments and comparisons with the field, the ratio  $\overline{u'^2}/\bar{u}^2$  can be taken

as  $0.2 \pm 0.03$ . For irregular streams, we can take  $\overline{D}_y = 0.6du^*$ . Substituting these values into (3.58) with  $I = 0.033$  gives the estimate

$$D_L = 0.011 \frac{\overline{u}^2 W^2}{du_*} \quad (3.60)$$

which has been found to agree with observations within a factor of 4 or so. Deviations are primarily due to factors not included in our analysis, such as recirculation and dead zones.

**Geomorphological estimates.** Deng et al. (2001) present a similar approach for an engineering estimate of the dispersion coefficient in straight rivers based on characteristic geomorphological parameters. The expression they obtain is

$$\frac{D_L}{hu_*} = \frac{0.15}{8\epsilon_{t0}} \left(\frac{W}{h}\right)^{5/3} \left(\frac{\overline{u}}{u_*}\right)^2 \quad (3.61)$$

where  $\epsilon_{t0}$  is a dimensionless number given by:

$$\epsilon_{t0} = 0.145 + \left(\frac{1}{3520}\right) \left(\frac{\overline{u}}{u_*}\right) \left(\frac{W}{h}\right)^{1.38} \quad (3.62)$$

These equations are based on the hydraulic geometry relationship for stable rivers and on the assumption that the uniform-flow formula is valid for local depth-averaged variables. Deng et al. (2001) compare predictions for this relationship and predictions from (3.60) with measurements from 73 sets of field data. More than 64% of the predictions by (3.61) fall within the range of  $0.5 \leq D_L|_{prediction}/D_L|_{measurement} \leq 2$ . This accuracy is on average better than that for (3.60); however, in some individual cases, (3.60) provides the better estimate.

**Dye studies.** One of the most reliable means of computing a dispersion coefficient is through a dye study, as illustrated in the applications of the next sections. It is important to keep in mind that since  $D_L$  is dependent on the velocity profile, it is, in general, a function of the flow rate. Hence, a  $D_L$  computed by a dye study for one flow rate does not necessarily apply to a situation at a much different flow rate. In such cases, it is probably best to perform a series of dye studies over a range of flow rates, or to compare estimates such as (3.60) to the results of one dye study to aid predictions under different conditions.

### 3.3 Application: Dye studies

The purpose of a dye tracer study is to determine a river's flow and transport properties; in particular, the mean advective velocity and the effective longitudinal dispersion coefficient. To estimate these quantities, we inject dye upstream, measure the concentration distribution downstream, and compare the results to analytical solutions. The two major types of dye injections are instantaneous injections and continuous injections. The following sections discuss typical results for these two injection scenarios.

### 3.3.1 Preparations

To prepare a dye injection study, we use engineering estimates for the expected transport properties to determine the location of the measurement station(s), the duration of the experiment, the needed amount of dye, and the type of dye injection.

For illustration purposes, assume in the following discussion that you measure a river cross-section to have depth  $h = 0.35$  m and width  $W = 10$  m. The last time you visited the site, you measured the surface current by timing leaves floating at the surface and found  $U_s = 53$  cm/s. A rule-of-thumb for the mean stream velocity is  $\bar{U} = 0.85U_s = 0.45$  cm/s. You estimate the river slope from topographic maps as  $S = 0.0005$ . The channel is uniform but has some meandering.

**Measurement stations.** A critical part of a dye study is that you measure far enough downstream that the dye is well mixed across the cross-section. If you measure too close to the source, you might obtain a curve for  $C(t)$  that looks Gaussian, but the concentrations will not be uniform across the cross-section, and dilution estimates will be biased. We use our mixing length rules of thumb to compute the necessary downstream distance.

Assuming the injection is at a point (conservative case), it must mix both vertically and transversely. The two relevant turbulent diffusion coefficients are

$$\begin{aligned} D_{t,z} &= 0.067d\sqrt{gdS} \\ &= 9.7 \cdot 10^{-4} \text{ m}^2/\text{s} \end{aligned} \quad (3.63)$$

$$\begin{aligned} D_{t,y} &= 0.6d\sqrt{gdS} \\ &= 8.7 \cdot 10^{-3} \text{ m}^2/\text{s}. \end{aligned} \quad (3.64)$$

The time it takes for diffusion to spread a tracer over a distance  $l$  is  $l^2/(12.5D)$ ; thus, the distance the tracer would move downstream in this time is

$$L_x = \frac{l^2}{12.5D}U. \quad (3.65)$$

There are several injection possibilities. If you inject at the bottom or surface, the dye must spread over the whole depth; if you inject at middle depth, the dye must only spread over half the depth. Similarly, if you inject at either bank, the dye must spread across the whole river; if you inject at the stream centerline, the dye must only spread over half the width. Often it is possible to inject the dye in the middle of the river and at the water surface. For such an injection, we compute in our example that  $L_{m,z}$  for spreading over the full depth is 4.2 m, whereas,  $L_{m,y}$  for spreading over half the width is 95 m. Thus, the measuring station must be at least  $L_m = 100$  m downstream of the injection.

The longitudinal spreading of the cloud is controlled by the dispersion coefficient. Using the estimate from Fischer et al. (1979) given in (3.60), we have

$$\begin{aligned} D_L &= 0.011 \frac{U^2W^2}{d\sqrt{gdS}} \\ &= 15.4 \text{ m}^2/\text{s}. \end{aligned} \quad (3.66)$$

We would like the longitudinal width of the cloud at the measuring station to be less than the distance from the injection to the measuring station; thus, we would like a Peclet number,  $Pe$ , at the measuring station of 0.1 or less. This criteria gives us

$$\begin{aligned} L_m &= \frac{D}{UPe} \\ &= 342 \text{ m.} \end{aligned} \quad (3.67)$$

Since for this stream the Peclet criteria is more stringent than that for lateral mixing, we chose a measurement location of  $L_m = 350 \text{ m}$ .

**Experiment duration.** We must measure downstream long enough in time to capture all of the cloud or dye front as it passes. The center of the dye front reaches the measuring station with the mean river flow:  $t_c = L_c/U$ . Dispersion causes some of the dye to arrive earlier and some of the dye to arrive later. An estimate for the length of the dye cloud that passes after the center of mass is

$$\begin{aligned} L_\sigma &= 3\sqrt{2D_L L_m/U} \\ &= 525 \text{ m} \end{aligned} \quad (3.68)$$

or in time coordinates,  $t_\sigma = 1170 \text{ s}$ . Thus, we should start measuring immediately after the dye is injected and continue taking measurements until  $t = t_c + t_\sigma = 30 \text{ min}$ . To be conservative, we select a duration of 35 min.

**Amount of injected dye tracer.** The general public does not like to see red or orange water in their rivers, so when we do a tracer study, we like to keep the concentration of dye low enough that the water does not appear colored to the naked eye. This is possible using fluorescent dyes because they remain visible to measurement devices at concentrations not noticeable to casual observation. The most common fluorescent dye used in river studies is Rhodamine WT. Many other dyes can also be used, including other types of Rhodamine (B, 6G, etc.) or Fluorescein. Smart & Laidlay (1977) discuss the properties of many common fluorescent dyes.

In preparing a dye study, it is necessary to determine the amount (mass) of dye to inject. A common field fluorometer by Turner Designs has a measurement range for Rhodamine WT of  $(0.04 \text{ to } 40) \cdot 10^{-2} \text{ mg/l}$ . To have good sensitivity and also leave room for a wide range of river flow rates, you should design for a maximum concentration at the measurement station near the upper range of the fluorometer, for instance  $C_{max} = 4 \text{ mg/l}$ .

The amount of dye to inject depends on whether the injection is a point source or a continuous injection. For a point source injection, we use the instantaneous point source solution with the longitudinal dispersion coefficient estimated above

$$\begin{aligned} M &= C_{max} A \sqrt{4\pi D_L L_m/U} \\ &= 5.4 \text{ g.} \end{aligned} \quad (3.69)$$

For a continuous injection, we estimate the dye mass flow rate from the expected dilution

$$\dot{m} = U_0 A_r C_{max}$$

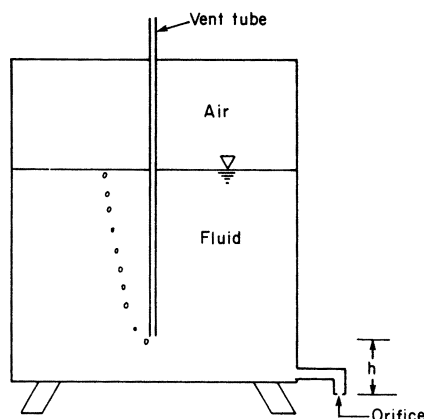


**Fig. 3.5.** Schematic of a Mariot bottle taken from Fischer et al. (1979).

$$= 6.3 \text{ g/s.} \quad (3.70)$$

These calculations show that a continuous release uses much more dye than a point release. These estimates are for the pure (usually a powder) form of the dye.

**Type of injection.** To get the best injection characteristics, we dissolve the powder form of the dye in a solution of water and alcohol before injecting it in the river. The alcohol is used to obtain a neutrally buoyant mixture of dye. For a point release, we usually spill a bottle of dye mixture containing the desired initial mass of dye in the center of the river and record the time when the injection occurs. For a continuous release, we require some tubing to direct the dye into the river, a reservoir containing dye at a known concentration, and a means of regulating the flow rate of dye.

The easiest way to get a constant dye flow rate is to use a peristaltic pump. Another means is to construct a Mariot bottle as described in Fischer et al. (1979) and shown in Figure 3.5. The idea of the Mariot bottle is to create a constant head tank where you can assume the pressure is equal to atmospheric pressure at the bottom of the vertical tube. As long as the bottle has enough dye in it that the bottom of the vertical tube is submerged, a constant flow rate  $Q_0$  will result by virtue of the constant pressure head between the tank and the injection. We must calibrate the flow rate in the laboratory for a given head drop prior to conducting the field experiment.

The concentration of the dye  $C_0$  for the continuous release is calculated according to the equation

$$\dot{m} = Q_0 C_0 \quad (3.71)$$

where  $Q_0$  is the flow rate from the pump or Mariot bottle. With these design issues complete, a dye study is ready to be conducted.

### 3.3.2 River flow rates

Figure 3.6 shows a breakthrough curve for a continuous injection, based on the design

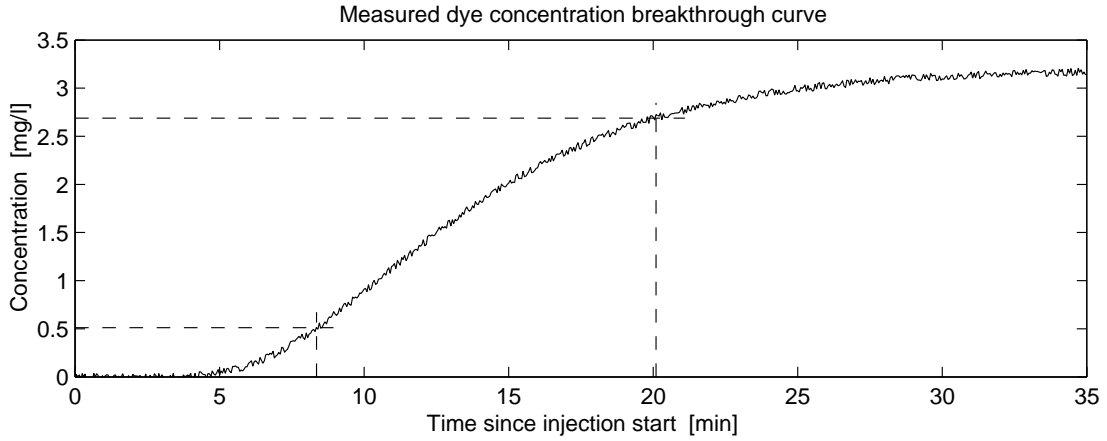


**Fig. 3.6.** Measured dye concentration for example dye study. Dye fluctuations are due to instrument uncertainty, not due to turbulent fluctuations.

in the previous section. The river flow rate can be estimated from the measured steady-state concentration in the river  $C_r$  at  $t = 35$  min. Reading from the graph, we have  $C_r = 3.15$  mg/l. Thus, the actual flow rate measured in the dye study was

$$\begin{aligned} Q_r &= \frac{\dot{m}}{C_r} \\ &= 2.0 \text{ m}^3/\text{s}. \end{aligned} \quad (3.72)$$

Notice that this estimate for the river flow rate is independent of the cross-sectional area.

To estimate the error in this measurement, we use the error-propagation equation

$$\delta\gamma = \sqrt{\sum_{i=1}^n \left( \frac{\partial\gamma}{\partial m_i} \delta m_i \right)^2} \quad (3.73)$$

where  $\delta\gamma$  is the error in some quantity  $\gamma$ , estimated from  $n$  measurements  $m_i$ . Computing the error for our river flow rate estimate, we have

$$\delta Q_r = \sqrt{\left( \frac{C_0}{C_r} \delta Q_0 \right)^2 + \left( \frac{Q_0}{C_r} \delta C_0 \right)^2 + \left( \frac{Q_0 C_0}{C_r^2} \delta C_r \right)^2}. \quad (3.74)$$

If the uncertainties in the measurements were  $C_r = (3.15 \pm 0.04)$  mg/l,  $C_0 = 32 \pm 0.01$  g/l and  $Q_0 = 0.2 \pm 0.01$  l/s, then our estimate should be  $Q_r = 2.0 \pm 0.1$  m<sup>3</sup>/s. The error propagation formula is helpful for determining which sources of error contribute the most to the overall error in our estimate.

### 3.3.3 River dispersion coefficients

The breakthrough curve in Figure 3.6 also contains all the information we need to estimate an *in situ* longitudinal dispersion coefficient. To do that, we will use the relationship

$$\sigma^2 = 2D_L t. \quad (3.75)$$

Since our measurements of  $\sigma$  are in time, we must convert them to space in order to use this equation. One problem is that the dye cloud continues to grow as it passes the site, so the width measured at the beginning of the front is less than the width measured after most of the front has passed; thus, we must take an average.

The center of the dye front can be taken at  $C = 0.5C_0$ , which passed the station at  $t = 12.94$  min and represents the mean stream velocity. One standard deviation to the left of this point is at  $C = 0.16C_0$ , as shown in the figure. This concentration passed the measurement station at  $t = 8.35$  min. One standard deviation to the right is at  $C = 0.84C_0$ , and this concentration passed the station at  $t = 20.12$  min. From this information, the average velocity is  $\bar{u} = 0.45$  m/s and the average width of the front is  $2\sigma_t = 20.12 - 8.35 = 11.77$  min. The time associated with this average sigma is  $t = 8.35 + 11.77/2 = 14.24$  min.

To compute  $D_L$  from (3.75), we must convert our time estimate of  $\sigma_t$  to a spatial estimate using  $\sigma = \bar{u}\sigma_t$ . Solving for  $D_L$  gives

$$\begin{aligned} D_L &= \frac{\bar{u}^2 \sigma_t^2}{2t} \\ &= 14.8 \text{ m}^2/\text{s}. \end{aligned} \tag{3.76}$$

This value compares favorably with our initial estimate from (3.50) of  $15.4 \text{ m}^2/\text{s}$ .

### 3.4 Application: Dye study in Cowaselon Creek

In 1981, students at Cornell University performed a dye study in Cowaselon Creek using an instantaneous point source of Rhodamine WT dye. The section of Cowaselon Creek tested has a very uniform cross-section and a straight fall line from the injection point through the measurement stations. At the injection site, the students measured the cross-section and flow rate, obtaining

$$\begin{aligned} Q &= 0.6 \text{ m}^3/\text{s} & W &= 10.7 \text{ m} \\ \bar{u} &= 0.17 \text{ m/s} & h &= 0.3 \text{ m}. \end{aligned}$$

From topographic maps, they measured the creek slope over the study area to be  $S = 4.3 \cdot 10^{-4}$ .

The concentration profiles were measured at three stations downstream. The first station was 670 m downstream of the injection, the second station was 2800 m downstream of the injection, and the final station was 5230 m downstream of the injection. At each location, samples were taken in the center of the river and near the right and left banks. Figure 3.7 shows the measured concentration profiles.

For turbulent mixing in the vertical direction, the downstream distance would be  $L_{m,z} = 12d = 17$  m. This location is well upstream of our measurements; thus, we expect the plume to be well-mixed in the vertical by the time it reaches the measurement stations.

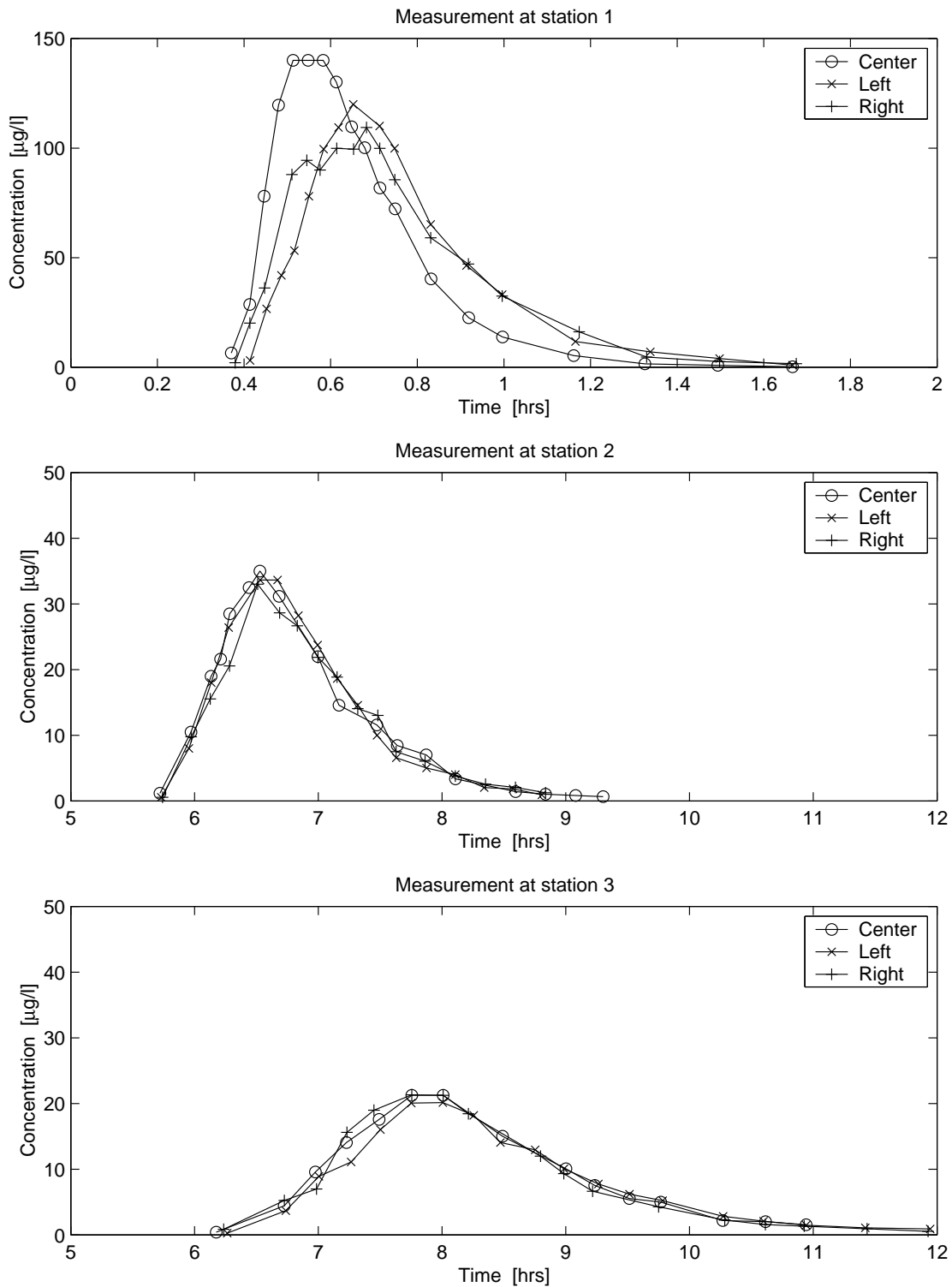


**Fig. 3.7.** Measured dye concentrations at two stations in Cowaselon Creek for a point injection. Measurements at each station are presented for the stream centerline and for locations near the right and left banks.

For mixing in the lateral direction, the method in Example Box 3.3 (using  $D_{t,y} = 0.15du_*$  for straight channels) gives a downstream distance of  $L_{m,y} = 2500$  m. Since the first measurement station is at  $L = 670$  m we clearly see that there are still lateral gradients in the concentration cloud. At the second measurement station, 2800 m downstream, the lateral gradients have diffused, and the lateral distribution is independent of the lateral coordinate. Likewise, at the third measurement station, 5230 m downstream, the plume is mixed laterally; however, due to dispersion, the plume has also spread more in the longitudinal direction.

To estimate the dispersion coefficient, we can take the travel time between the stations two and three and the growth of the cloud. The travel time between stations is  $\delta t = 3.97$  hr. The width at station one is  $\sigma_1 = 236$  m, and the width at station two is  $\sigma_2 = 448$  m. The dispersion coefficient is

$$\begin{aligned} D_L &= \frac{\sigma_2^2 - \sigma_1^2}{2\delta t} \\ &= 5.1 \text{ m}^2/\text{s}. \end{aligned} \tag{3.77}$$

Comparing to (3.60) and (3.61), we compute

$$D_L|_{Fischer} = 3.3 \text{ m}^2/\text{s} \tag{3.78}$$

$$D_L|_{Deng} = 5.4 \text{ m}^2/\text{s}. \tag{3.79}$$

Although the geomorphological estimate of  $5.4 \text{ m}^2/\text{s}$  is closer to the true value than is  $3.3 \text{ m}^2/\text{s}$ , for practical purposes, both methods give good results. Dye studies, however, are always helpful for determining the true mixing characteristics of rivers.

## Summary

This chapter presented the effects of contaminant transport due to variability in the ambient velocity. In the first section, turbulence was discussed and shown to be composed of a mean velocity and a random, fluctuating turbulent velocity. By introducing the Reynolds decomposition of the turbulent velocity into the advective diffusion equation, a new equation for turbulent diffusion was derived that has the same form as that for molecular diffusion, but with larger, turbulent diffusion coefficients. The second type of variable velocity was a shear velocity profile, described by a mean stream velocity and deterministic deviations from that velocity. Substituting a modified type of Reynolds decomposition for the shear profile into the advective diffusion equation and depth averaging led to a new equation for longitudinal dispersion and an integral relationship for calculating the longitudinal dispersion coefficient. To demonstrate how to use these equations and obtain field measurements of these properties, the chapter closed with an example of a simple dye study to obtain stream flow rate and longitudinal dispersion coefficient.

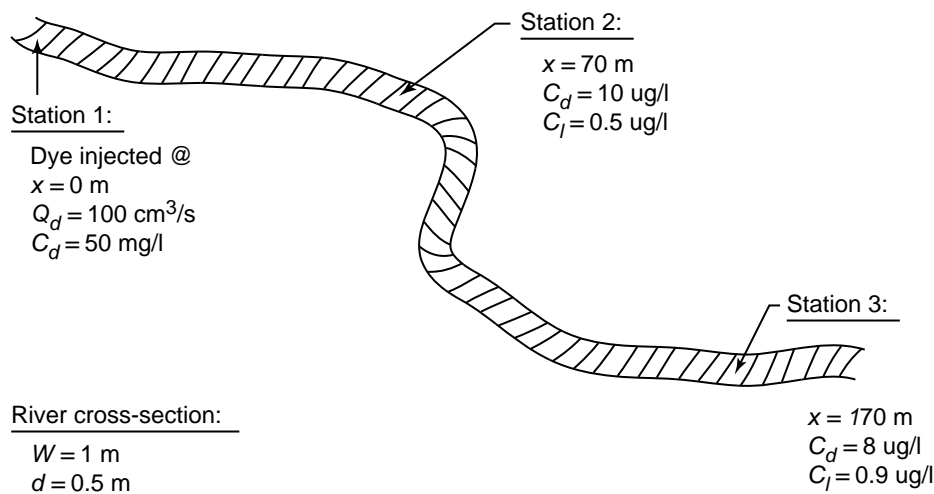


Fig. 3.8. Schematic data for the Lindane contamination dye study problem.

## Exercises

**3.1** Turbulent diffusion coefficients. What are the vertical and transverse diffusion coefficients for the Rhein river in the vicinity of Karlsruhe? How long will it take for a contaminant discharged at the river edge to be fully mixed vertically? laterally?

**3.2** Numerical integration. Using the velocity profile data in Table 3.1 (from Nepf (1995)), perform a numerical integration of (3.53) to estimate a longitudinal dispersion coefficient. You should obtain a value of  $D_L = 1.5 \text{ m}^2/\text{s}$ .

**3.3** Dye study (taken from Nepf (1995)). A small stream has been found to be contaminated with Lindane, a pesticide known to cause convulsions and liver damage. Groundwater wells in the same region have also been found to contain Lindane, and so you suspect that the river contamination is due to groundwater inflow. To test your theory, you conduct a dye study. Based on the information given in Figure 3.8, what is the groundwater volume flux and the concentration of Lindane in the groundwater? Due to problems with the pump, the dye flow rate has an error of  $\pm 5 \text{ cm}^3/\text{s}$ . Assume this is the only error in your measurement and report your measurement uncertainty.

**Table 3.1.** Stream velocity data for calculating a longitudinal dispersion coefficient.

Station number	Distance from bank [cm]	Total depth $d$ [cm]	Measurement depth, $z/d$ [-]	Velocity $u$ [cm/s]
1	0.0	0	0	0.0
2	30.0	14	0.6	3.0
3	58.4	42	0.2	6.0
			0.8	6.4
4	81.3	41	0.2	16.8
			0.8	17.6
5	104.1	43	0.2	13.4
			0.8	13.6
6	137.2	41	0.2	13.6
			0.8	14.2
7	170.2	34	0.2	9.0
			0.8	9.6
8	203.2	30	0.2	5.0
			0.8	5.4
9	236.2	15	0.2	1.0
			0.8	1.4
10	269.2	15	0.2	0.8
			0.8	1.2
11	315.0	14	0.6	0.0
12	360.7	0	0	0.0